Original Article

JCBFM

Journal of Cerebral Blood Flow & Metabolism
2020, Vol. 40(9) 1778–1796

DOI: 10.1177/0271678X19877889
journals.sagepub.com/home/jcbfm
SAGE

Experimental cortical stroke induces aberrant increase of sharp-wave-associated ripples in the hippocampus and disrupts cortico-hippocampal communication

Ji-Wei He[1,2,*], Gratianne Rabiller[1,2,*], Yasuo Nishijima[1,2,3], Yosuke Akamatsu[1,2,3], Karam Khateeb[4], Azadeh Yazdan-Shahmorad[4,5] and Jialing Liu[1,2]

Abstract

The functional consequences of ischemic stroke in the remote brain regions are not well characterized. The current study sought to determine changes in hippocampal oscillatory activity that may underlie the cognitive impairment observed following distal middle cerebral artery occlusion (dMCAO) without causing hippocampal structural damage. Local field potentials were recorded from the dorsal hippocampus and cortex in urethane-anesthetized rats with multichannel silicon probes during dMCAO and reperfusion, or mild ischemia induced by bilateral common carotid artery occlusion (CCAO). Bilateral change of brain state was evidenced by reduced theta/delta amplitude ratio and shortened high theta duration following acute dMCAO but not CCAO. An aberrant increase in the occurrence of sharp-wave-associated ripples (150–250 Hz), crucial for memory consolidation, was only detected after dMCAO reperfusion, coinciding with an increased occurrence of high-frequency discharges (250–450 Hz). dMCAO also significantly affected the modulation of gamma amplitude in the cortex coupled to hippocampal theta phase, although both hippocampal theta and gamma power were temporarily decreased during dMCAO. Our results suggest that MCAO may disrupt the balance between excitatory and inhibitory circuits in the hippocampus and alter the function of cortico-hippocampal network, providing a novel insight in how cortical stroke affects function in remote brain regions.

Keywords

Local field potential, phase amplitude coupling, modulation index, connectivity, distal middle cerebral artery occlusion, common carotid artery occlusion

Received 8 April 2019; Revised 22 July 2019; Accepted 25 July 2019

Introduction

Stroke afflicts 800,000 people per year and has become the leading cause of adult disability in the US. Apart from sensory and motor impairment, post-stroke cognitive impairment in various domains from attention deficits to memory problems is not uncommon.[1–3] The hippocampus is involved in memory function, but direct ischemic lesions strategic to the hippocampus or parahippocampal regions are rarely observed in middle cerebral artery (MCA) stroke.[4–6] Consistent with clinical observation, cognitive impairment can be detected in animal models of stroke in the absence of

[1]Department of Neurological Surgery, UCSF, San Francisco, CA, USA
[2]Department of Neurological Surgery, SFVAMC, San Francisco, CA, USA
[3]Department of Neurosurgery, Tohoku University Graduate School of Medicine, Sendai, Japan
[4]Departments of Bioengineering and Electrical and Computer Engineering, University of Washington, Seattle, WA, USA
[5]Center for Integrative Neuroscience and Department of Physiology, University of California, San Francisco, CA, USA

*These authors contributed equally to the work.

Corresponding author:
Jialing Liu, Department of Neurological Surgery (112C), University of California at San Francisco and Department of Veterans Affairs Medical Center, 1700 Owens Street, San Francisco, CA 94158, USA.
Email: jialing.liu@ucsf.edu

hippocampal injury.[7,8] However, the neural changes in the hippocampus that may underlie the functional impairment induced by cortical stroke are not well understood.

Stroke leads to down regulation in the GABAergic transmission,[9,10] changes in connectivity among functional networks between the cortex and hippocampus[11,12] as well as a host of changes in brain oscillations serving to communicate between brain networks,[13,14] all of which can potentially affect brain regions remote to stroke. For example in the hippocampus, the firing of sharp-wave-associated ripples (SWRs), a high-frequency activity in the pyramidal layer[15] that requires temporally precise local interactions between excitatory and inhibitory neurons in the CA1,[16–18] can potentially be disrupted by MCAO that alters GABA receptor expression.[9] The selective elimination of SWRs during post-learning sleep resulted in impairment of memory,[19,20] suggesting that the dysregulation of SWRs may interfere with memory consolidation and transferring memory from the hippocampus to cortex. A second potential target of MCAO can be the theta rhythm, a nearly sinusoidal oscillation at 4–7 Hz originated from the hippocampus, not only correlates with memory performance but also is involved in memory consolidation during REM sleep.[21,22] Conversely, the hippocampal non-theta state, also known as the slow wave state (SWS), is associated with immobility or SWS sleep.[23,24] Manipulating the hippocampal theta rhythm alters cognition, further suggesting a causal role of the hippocampal theta in cognition.[25,26] The third likely target, cortical gamma oscillations, including low- (30–60 Hz) and high gamma oscillations (60–150 Hz), are known to play a role in sensory stimulation,[27,28] declarative memory,[29] attentional selection,[30] cognition,[31] and assist in encoding and retrieval of memory traces in the hippocampal formation.[32–34] Ample evidence suggests that theta oscillations provide a temporal reference for the exchange of information among different brain networks, whereas faster gamma-frequency oscillations nested within theta cycles underlie local information processing in the cortex.[35,36] Thus, hippocampal theta-gamma coupling, in which gamma oscillations are modulated by theta oscillations, is stronger during memory replay. Conversely, poor hippocampal coupling between theta and gamma could predict poor memory performance.[37,38] Likewise, reduced modulation of cortical gamma amplitude during hippocampal theta phase was detected in a mouse model of Alzheimer's Disease with cognitive deficit,[39] and in schizophrenic patients associated with working memory dysfunction.[40]

The perturbation of brain oscillations occurs in response to the reduction of cerebral blood flow (CBF) and energy deprivation, resulting in decreased amplitude in high-frequency rhythms in electroencephalography (EEG) and increased power in slower frequency rhythms.[13,41] Yet little is known about the dynamics of hippocampal oscillations in the course of brain ischemia and how they respond to critical dip of CBF that causes irreversible neuronal damage in the cortex, leading to the disruption of connectivity between cortex and the other brain networks including the hippocampal formation.[11] Changes in the inhibitory and excitatory neurotransmitter systems have been well documented in the motor cortex after stroke[42,43]; however, little is known regarding how they change other remote brain regions such as the hippocampus and their effects on neuronal activity. The current study sought to determine how distal MCA stroke affected cortical and hippocampal oscillatory activity. Our results indicate that ischemic stroke in the cortex profoundly affects multiple hippocampal oscillations, among which the dysregulation of SWRs and the altered theta-gamma modulation may contribute to cognitive impairment post stroke.

Methods and materials

Animals and housing

All experiments were conducted in accordance with the Guide for Care and Use of Laboratory Animals (National Research Council. 2011. Guide for the Care and Use of Laboratory Animals: Eighth Edition. Washington, DC), reported in compliance with the Animals in Research: Reporting In Vivo Experiments (ARRIVE) guidelines, and were approved by the San Francisco VA Medical Center Institutional Animal Care and Use Committee (IACUC). A total of 24 adult male Sprague-Dawley rats approximately 2.5 months of age weighing 250 g were purchased from Charles River Laboratories (Wilmington, MA) and housed in institutional standard cages (two rats per cage) on a 12-h light/12-h dark cycle with ad libitum access to food and water before the experimental procedures. The identity of the test subject was blinded to investigators who performed the stroke surgery and electrophysiology recording and who analyzed the data.

Experimental stroke

Stroke was induced unilaterally in rats by the distal middle cerebral artery occlusion (dMCAO) method in combination with supplemental proximal artery occlusion of the bilateral common carotid arteries (CCAO) under isoflurane (1.5%)/O_2(30%)/N_2O(68.5%) anesthesia as described previously,[44] producing cortical infarct restricted to the somatosensory (SS) cortex in

the absence of direct hippocampal injury.[8] In brief, a 1.5 mm diameter burr hole 1 mm rostral to the anterior junction of the zygoma and temporalis bone was made with a dental drill. The dura mater was carefully pierced with a 30-gauge needle. The main trunk of the left MCA was ligated permanently above the rhinal fissure with a 10–0 suture, and the bilateral common carotid arteries (CCA) were occluded temporarily for 60 min with 4–0 sutures. The sutures were then removed to restore blood flow, and the cervical incision was closed. Core temperature was maintained at 37 ± 0.5°C with a heating blanket and rectal thermistor servo-loop throughout the procedure. Due to the well-known effect of reduced CBF on brain EEG rhythms, an additional cohort of rats with temporary bilateral CCAO was included to differentiate the effect of temporary CBF reduction from permanent cortical infarct on brain oscillations.

Recording

Electrophysiological recordings were performed using multisite extracellular silicon probes (NeuroNexus Technologies) under urethane anesthesia for 2 h (Sigma, 15 mg/kg i.p.) as described.[8,45] Following craniotomy, two electrodes (A1x32-6mm-50-177 into the ipsilateral side and A1x16-5mm-100-703 into the contralateral side, respectively) were slowly inserted into the brain after the dura mater was resected to target the dorsal hippocampus at (AP: −3.3 mm; ML: ± 2 mm) via a stereotaxic frame (David Kopf Instruments, Tujunga, CA, USA). The electrode and recording sites in the brain are shown in Figure 1(a) to (c). Real-time data display and an audio aid were used to facilitate the identification of proper recording location while advancing electrodes until characteristic signals from stratum pyramidale and stratum radiatum were detected and recorded. A 2-h multi-channel recording from bilateral sensorimotor cortex and dorsal hippocampus was collected from each rat. Data were stored at a sampling rate of 32 kHz after band-pass filtering (0.1–9 kHz) with an input range of ± 3 mV (Digital Lynx SX, Neuralynx, USA). Approximately 10% rats died during recording, and the data were excluded from analysis.

Tissue preparation and infarct assessment

One to 1.5 h after dMCAO reperfusion, rats were perfused transcardially with 4% PFA in 0.1 M phosphate buffer, pH 7.4. The brains were collected, post fixed overnight in 4% PFA and placed in 30% sucrose solution for 24 h. Brains were cut coronally in 40 um-thick sections and stored at 4°C. Serial coronal sections were stained using the hematoxylin and eosin (H&E) method. Infarct volume was measured by subtracting the volume of intact tissue in the ipsilateral side from that in the contralateral side using Stereoinvestigator software (Microbrighfield, VA).[46]

Analysis

Prior to data processing, the precise locations of the pyramidal and radiatum layers were confirmed manually by using off-line analysis software (Neuroscope, GNU) with respect to unit activity, sharp waves and SWRs. Prior to quantification, all recordings were initially band-pass filtered at 0.1–9 K Hz with an input range of ± 3 mV (Digital Lynx SX, Neuralynx, USA) and down-sampled to 1250 Hz (Matlab, MathWorks, USA). Occasionally, data conversion failed in this step in one or more channels due to low-quality recordings, resulting in missing data in affected channels. Only rats with complete down-sampled data for all channels and with all-time points were included in the analysis. SWRs and high-frequency discharges (HFDs) events were analyzed from CA1 pyramidal layer of the hippocampus. For the analysis of hippocampal recordings and theta state selection, data from the stratum lacunosum moleculare (slm) layer were selected over other layers for the main analyses based on the high signal-to-noise ratio in slm (Figure 1(d) to (i)).[47,48]

Local field potentials (LFPs) were band-pass filtered for the following frequency bands: theta (4–7 Hz), delta (0.1–3 Hz), low gamma (LoG: 30–60 Hz) and high gamma (HiG: 60–150 Hz). Regarding brain state detection, two states of high theta/delta (HTD) and low theta/delta (LTD) were defined by first calculating Hilbert amplitudes for both frequency bands in slm.[49–51] The amplitude envelopes were then smoothed with a Gaussian kernel ($\sigma = 1$ s, 8 s window) and the ratio of hippocampal theta to delta band amplitude (T/D) was calculated. The result was then convolved with a smoothing Gaussian kernel ($\sigma = 10$ s, 80 s window), after which a manually set threshold ratio was used to capture sustained HTD and LTD periods.

Periods of SWRs and HFDs were detected from the smoothed LFPs following Hilbert transformation (150–250 Hz for SWRs; 250–450 Hz for HFDs) of recordings in the CA1 pyramidal layer. SWRs and HFDs were defined as periods in which the smoothed envelope exceeded a threshold amplitude six times greater than the baseline standard deviation for at least 15 ms. SWRs and HFDs were analyzed only during LTD (non-theta state or SWS) period per previous method.[52] The average occurrence of events was examined between baseline, occlusion and reperfusion periods. Occurrence of events was derived by dividing the numbers of events by the duration of LTD period (in seconds).

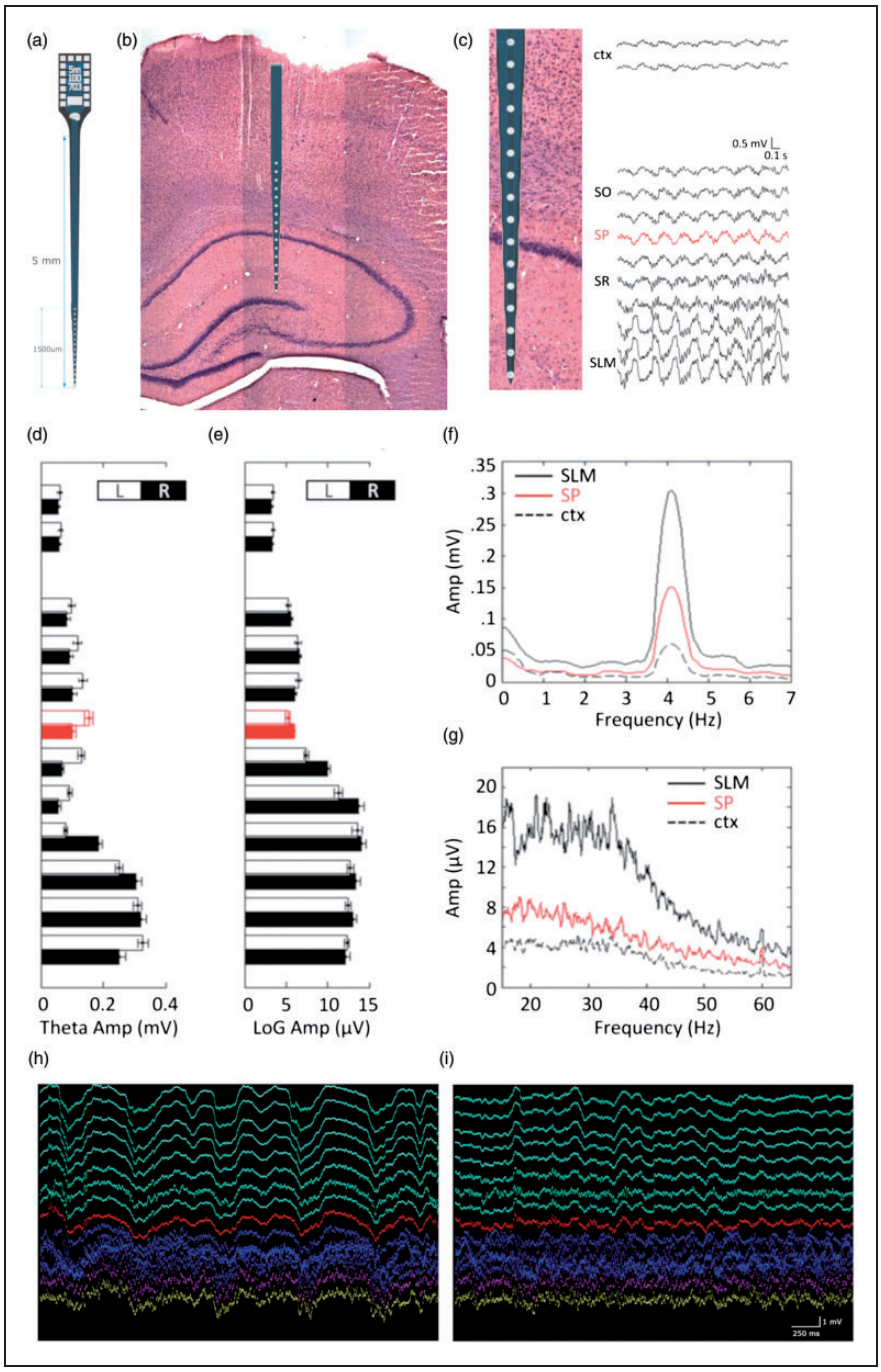

Figure 1. The amplitude of theta oscillation peaks at the stratum lacunosum moleculare. (a) Schematic representation of the A1x16-5mm-100-703 Neuronexus probe. (b) An example of the H&E-stained brain section showing the probe location with the corresponding channels spanning the brain layers. (c) Local field potential traces of a 2-s multichannel recording spanning from the cortex (top two traces) to the hippocampus (bottom traces) using a 16-channel NeuroNexus probe in a urethane-anesthetized rat without vessel occlusion. Anatomical structure corresponding to each channel is labeled as cortex (ctx), stratum oriens (so), stratum pyramidale (sp- trace labeled in red), stratum radiatum (sr) and stratum lacunosum moleculare (slm). In the frequency domain, theta- (d: max between 3 and 7 Hz) and low gamma-band (e: LoG; median between 20 and 50 Hz) amplitudes for each channel were computed. White (L: left) and black (R: right) bars: simultaneous bilateral recording within the same animal ($N = 12$). Mean spectrograms of the pyramidal layer channels (red), one cortical channel (dotted black), and one molecular layer channel (solid black) are shown for theta (f) and low gamma (g). Typically, the slm channels chosen for analysis are located 400–600 μm below the pyramidal layer. (i–h), 5000 ms representative traces of multichannel recording during Low-theta/delta (h) state and high-theta/delta state (i). Green channels label the cortical layers, red channel the pyramidal layer of the CA1 and purple channel the stratum lacunosum moleculare layer. Scale bar: 250 ms and 1 mv.

To determine phase-amplitude coupling between hippocampal theta and cortical gamma oscillations, the modulation index (MI) was calculated using the algorithm described previously.[53] Briefly, either the slm layer or CA1 pyramidal layer were used to analyze the hippocampal theta phase coupling with the cortical gamma amplitude during HTD periods. In particular, band-pass filters for low gamma (LoG) and high gamma (HiG) were set at 30–60 Hz and 60–150 Hz, respectively. A Hilbert transform was applied to obtain the amplitude time series of the cortical LFPs and the phase time series of the hippocampal LFPs. To determine the MI, the phase time series were grouped into 18 bins, wherein the mean amplitude for each phase bin was calculated and standardized over the sum of all mean amplitudes.

Statistical analyses

Data are expressed as mean ±SD. For data with a normal distribution, as tested with Kolmogorov–Smirnoff tests (GraphPad Prism, v5.00), one-way ANOVA was performed to assess the main effect of acute dMCAO or CCAO on each variable. Post hoc Bonferroni's multiple comparisons were used to characterize the temporal profile. Student's *t* test was used to assess the lateralization effect. For non-normal distributed data sets, nonparametric tests were applied; e.g. Friedman test for multiple comparisons of paired samples, and Kruskal–Wallis test for multiple comparisons of independent samples followed by a post hoc Dunn's Multiple Comparison test. *P* values less than 0.05 were considered as significant.

Results

Cortical ischemic stroke increases the occurrence of hippocampal SWRs and HFDs

To determine whether cortical stroke affects the synchrony of the hippocampal circuit by altering the interplay between excitation and inhibition, we recorded neural activity as LFPs from different depths starting at deep cortical layers down to the hippocampus in rats under urethane anesthesia and analyzed the occurrence of SWRs. Consistent with previous findings, SWRs were detected in the pyramidal layer and accompanied by sharp waves in the stratum radiatum (Figure 2(a) and (b)). There were few ripple events taking place during baseline due to the predominance of theta brain state in this period. In contrast, there was a significant increase in the rate of ripple occurrence during ischemic reperfusion of dMCAO compared to baseline in both the ipsilateral and contralateral CA1 (Figure 2(c)). Unlike dMCAO, mild ischemia via temporary CCAO did not alter SWRs occurrence even during the periods when the duration of SWSs was increased. Besides SWRs, the occurrence of HFDs in the range of 250–450 Hz was also increased during ischemic reperfusion following dMCAO but not CCAO (Figure 2(d)), resulting in the increased proportion of HFDs in the pathological range compared to the physiological range of ripples (Figure 2(e)).

Under urethane anesthesia, dMCAO produced an ischemic lesion mainly in the somatosensory cortex (Figure 2(f)), a location similar to that seen under isoflurane anesthesia.[8,44] Infarct volume determined at 1–1.5 h after reperfusion was $24.85 \pm 7.50\,mm^3$, significantly smaller than the lesion size observed at five to seven weeks after dMCAO in our previous studies.[44]

Cerebral ischemia alters brain states in the hippocampus

Because an increased duration of the delta brain state is often associated with adverse neurological function[54,55] and T/D amplitude ratio is regarded as a potential biomarker of post-stroke cognitive outcome,[56] we thus examined the effect of cerebral ischemia on brain states. Since LFP data recorded in the slm layer displayed the most robust signal-to-noise ratio in theta amplitude compared to those recorded in the stratum pyramidal layer or cortical layers (Figure 1(d) to (g)), this layer was selected as the main source of the hippocampal data for theta-related studies. Despite the greatest changes in LFP power occurring immediately following the occlusion of MCA or CCAs, statistical comparisons were made only during the second half of the occlusion period due to incomplete recording among rats that underwent dMCAO procedures.

We found that during baseline recording, the hippocampus is dominated by the HTD state (Figure 3(a)). However, HTD duration was reduced following CCAO in the bilateral hippocampi and following dMCAO in the ipsilateral hippocampus. CCAO also increased the frequency of altering states between HTD and LTD by shortening the duration of each state, as demonstrated by a temporary but significant increase in the number of discontinuing HTD periods during CCAO in contralateral hemisphere (Figure 3(b)). Although T/D amplitude ratio tended to reduce after mild cerebral ischemia by CCAO, a significant and greater reduction of T/D amplitude ratio was found only after dMCAO and persisted throughout ischemic reperfusion (Figure 3(c)). The prolonged decrease in the hippocampal T/D amplitude ratio following dMCAO is reminiscent of the delta predominance, i.e. a typical feature in non-theta state, frequently observed in human EEG recording near infarct shortly after stroke onset,[57] suggesting

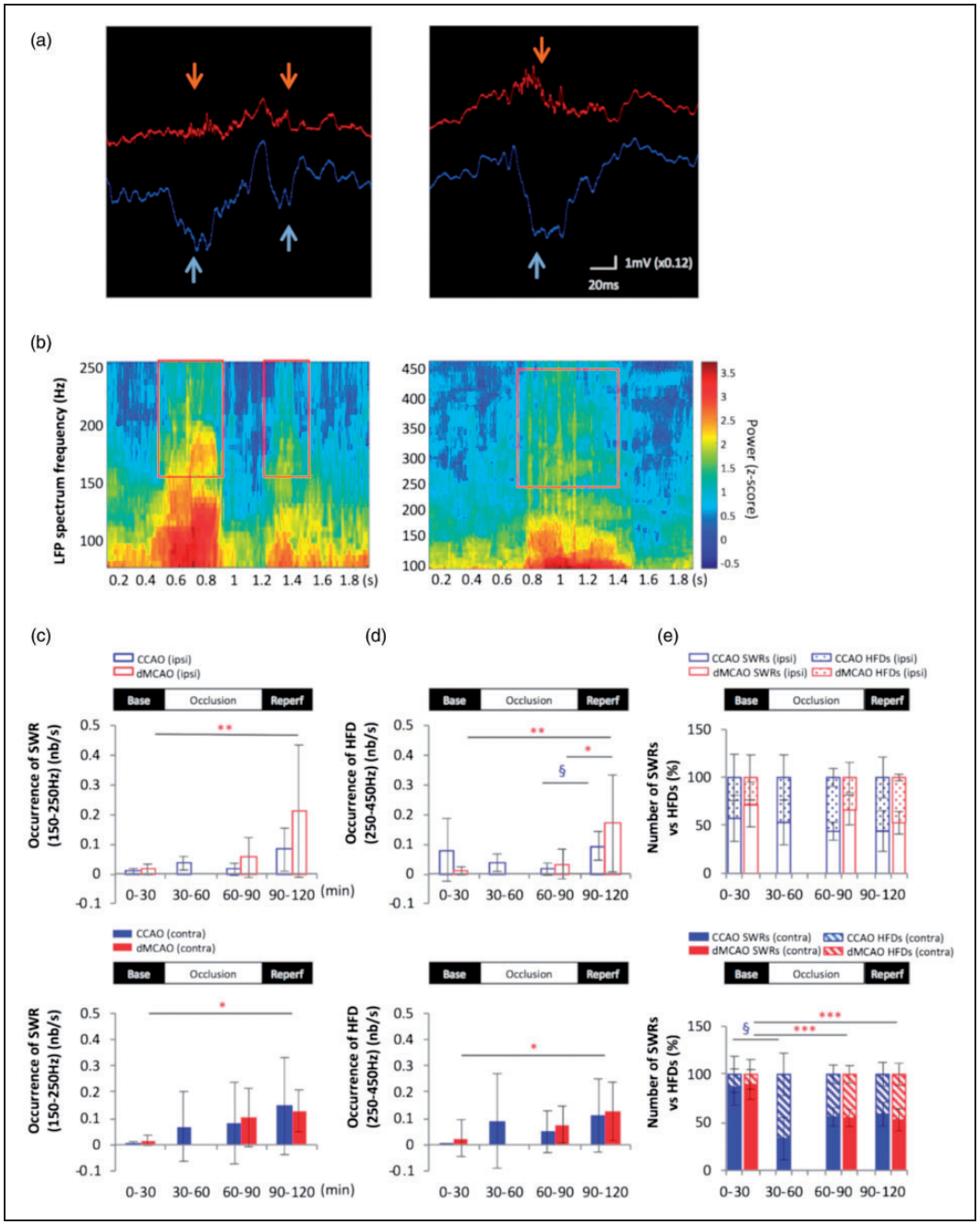

Figure 2. Cortical stroke increases the occurrence of sharp-wave-associated ripples and high-frequency discharges in the hippocampus. (a) Selective traces of local field potential (LFP) during baseline (left) and dMCAO reperfusion (right) period recorded in the ipsilateral CA1 pyramidal layer (red) and the stratum radiatum layer 200 mm below (blue). Each sharp wave event in the radiatum (light blue arrows) was associated with high-frequency oscillations, also known as the sharp-wave-associated ripples (SWRs) (orange arrows) in the CA1 pyramidal layer. Increased occurrence of SWRs with longer duration is often observed during reperfusion of dMCAO compared to those during baseline. (b) Frequency spectrograms of the LFP recording from CA1 pyramidal layer during dMCAO display the presence of physiological SWRs in the frequency range of 150–250 Hz (left) and the high-frequency discharges in the range of 250–450 Hz embedded in the ripple discharges (right), corresponding to traces in the left and right panel in A, respectively. An increase in the occurrence of SWRs (150–250 Hz) (c) and HFDs (250–450 Hz) (d) was detected in the bilateral CA1 pyramidal layers during MCA reperfusion compared to baseline in the bar graphs, respectively (ipsilateral: open bar panel; contralateral: solid bar panel). (e) A relative increase in HFDs to SWRs was observed in the contralateral CA1 during occlusion and reperfusion of dMCAO. In contrast, CCAO did not increase either SWRs or HFDs occurrence during reperfusion but only transiently increased the numbers of HFDs relative to SWRs in the contralateral CA1 pyramidal layer during the first 30 min of occlusion. $^{*}p < 0.05$, $^{**}p < 0.01$, $^{***}p < 0.001$ (for dMCAO); $^{\S}p < 0.05$ (for CCAO) for multiple comparisons between baseline and other levels. dMCAO: N = 10; CCAO: N = 7. (f) Hematoxylin and eosin (H&E)-stained coronal brain sections of a stroked rat showing the infarct area (black arrows). The volume of the infarct is $24.85 \pm 7.50\,mm^3$ or $5.36 \pm 0.99\%$ of the ipsilateral hemisphere (N = 4). Tissue was collected 1–1.5 h after reperfusion. (g) Higher magnification of the ipsilateral infarct area and contralateral homotopic area in the cortex. The red arrow shows the pnykotic nucleus of an apoptotic cell. Scale bars are 100 um for magnification × 10 and 20 um for magnification × 40.

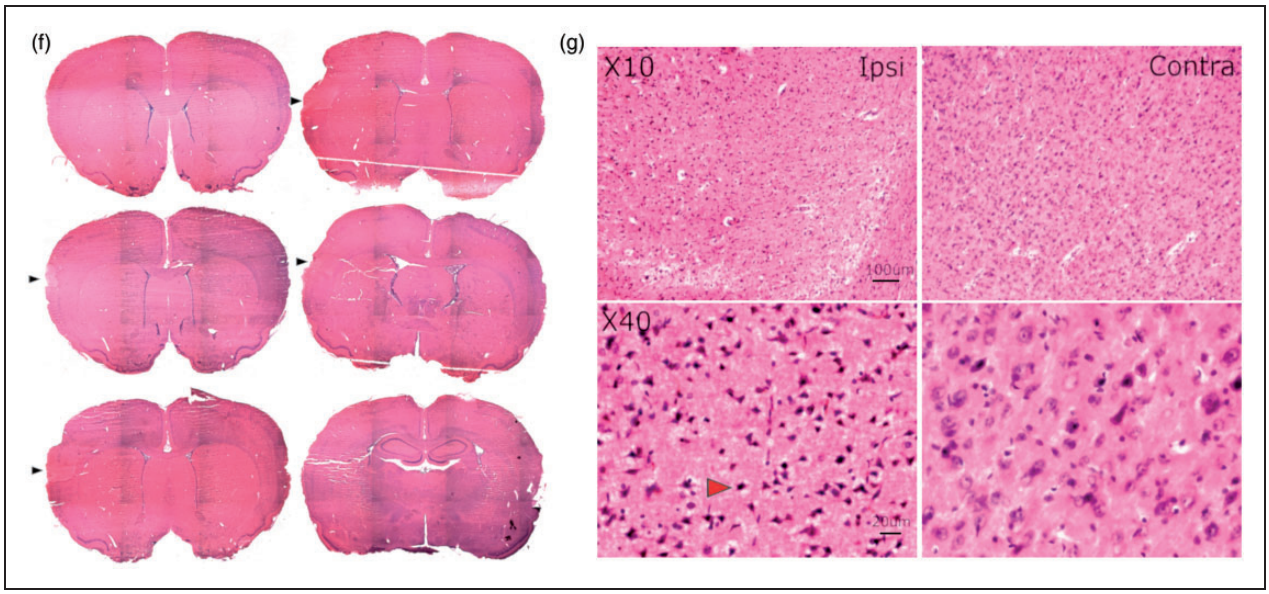

Figure 2. Continued.

that ischemic stroke might potentially affect neural activity of brain regions beyond the cortex.

Cortical ischemic stroke temporarily impacts hippocampal theta and gamma oscillations

Because a wealth of literature suggests that the reduction of cerebral blood flow results in the decrease or loss in EEG amplitude and frequency,[13,14,57] we next determined whether brain ischemia affected oscillations in the hippocampus that is remote from the ischemic core. We found that the delta power was only transiently increased for less than 5 min in the hippocampal slm layer following an episode of mild ischemia via bilateral CCAO; interestingly, it normalized quickly likely due to the robust collateral flow compensation via the circle of Willis.[58] Similar changes in delta power were detected in the contralateral hippocampus (Figure 4).

Specifically during the HTD phase, a temporary reduction of theta and gamma power was detected bilaterally in the hippocampal slm during dMCAO period (Figure 4(c) and (d)). Theta and gamma power was most affected during the initial period of occlusion, while gradually restored during ischemic reperfusion (Figure 4). However, despite the gradual recovery of bilateral hippocampal oscillations towards baseline level, the power of delta, theta and gamma exhibited great fluctuations during ischemic reperfusion of dMCAO, suggesting a lasting effect of stroke on brain oscillations (Figure 4(a) and (b)).

A similar reduction of theta and gamma power was also observed in the contralateral CA1 field of the hippocampus only after dMCAO (Figure 5). CCAO induced a transient increase in delta power in ipsilateral CA1 during the first 30 min of occlusion period, further suggesting that hippocampal blood flow was only impacted for a very brief period of time during ischemia.

dMCAO alters cortical gamma amplitude coupled to the hippocampal theta phase

In light of the significance of cross-frequency coupling between oscillations in network communication and information exchange, we investigated the dynamics of theta–gamma interactions during acute ischemia in simultaneous recordings from the hippocampus and cortex. We found that two distinct gamma bands in the cortex displayed dynamic and differential phase-amplitude modulation. There was an increase in the modulation index between cortical high gamma band and hippocampal theta (4–7 Hz) ($MI_{HiG\text{-}theta}$) or low frequency oscillations (0–4 Hz) ($MI_{HiG\text{-}Lowfreq}$) during MCA occlusion and reperfusion period in the ipsilateral CA1 layer during HTD phase (Figure 6(a), (c) and (e)). Increased coupling of cortical low gamma and hippocampal low frequency oscillations ($MI_{LoG\text{-}Lowfreq}$) was observed during MCA occlusion in bilateral CA1 (Figure 6(a), (c) and (e)). Interestingly, the main high gamma activity appeared to be coupled to the phase of delta wave oscillation during MCA occlusion, which further shifted towards lower frequencies (<1.5 Hz) during reperfusion. Increased MI_{HiG} in theta and low frequencies phases was also detected in the ipsilateral slm layer during dMCAO occlusion period

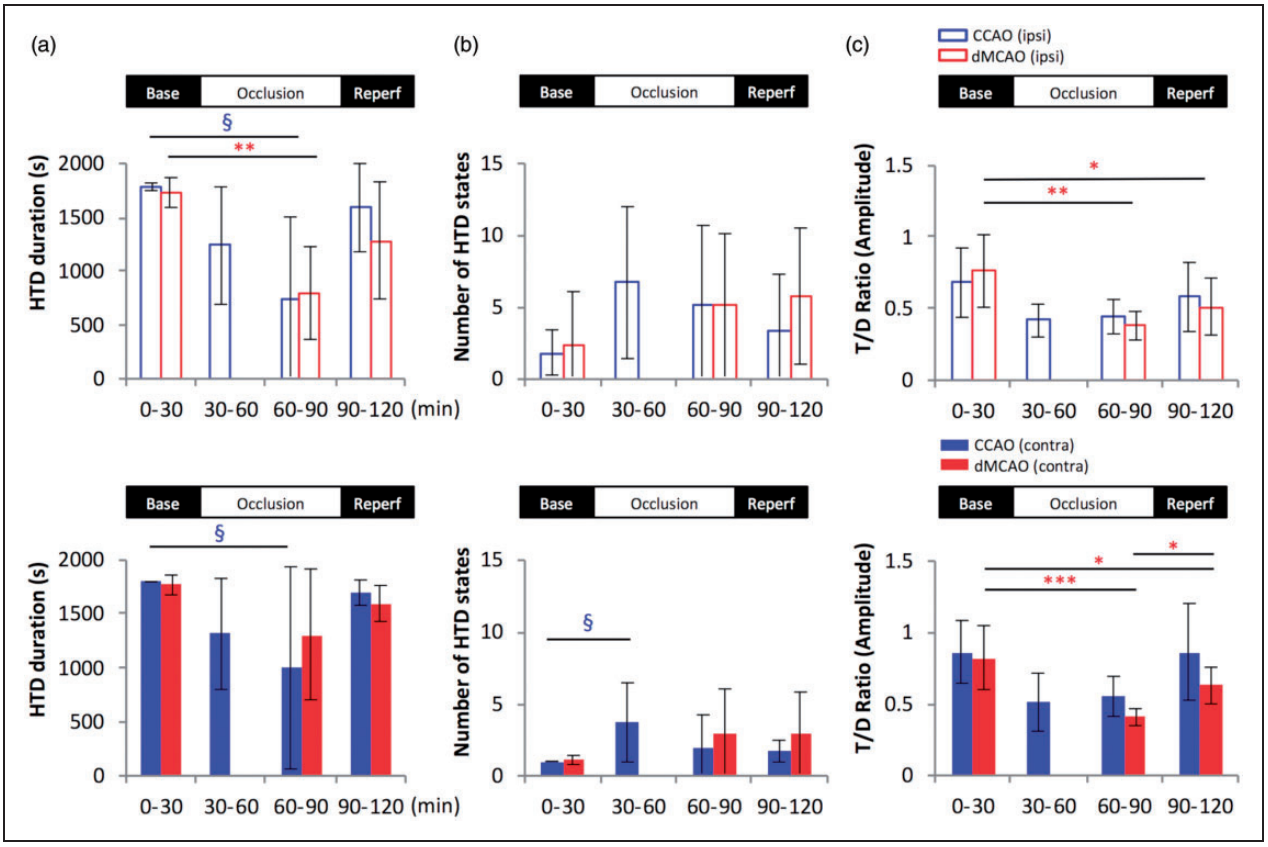

Figure 3. Cerebral ischemia reduces high theta state duration and decreases theta/delta ratio. The total duration of high theta/delta brain states was summed for each 30-min period in the ipsilateral- (upper panel with open bars) and contralateral (lower panel with solid bars) hippocampus slm layers for rats subjected to CCAO (blue) or dMCAO (red). (a) A temporary decrease in the HTD duration was detected during both dMCAO and CCAO occlusion period compared to baseline. (b) A significant increase in the transition between HTD and LTD, expressed as the number of HTD states, was observed during the first 30 min of CCAO occlusion in the contralateral hippocampus. (c) T/D ratio was decreased in the bilateral slm during dMCAO but not CCAO occlusion and persisted during ischemic reperfusion compared to baseline period. $^{*}p < 0.05$, $^{**}p < 0.01$, $^{***}p < 0.001$ (for dMCAO); $^{\S}p < 0.05$ (for CCAO) for multiple comparisons between baseline and other levels. dMCAO: N = 10; CCAO: N = 7.

(Figure 7(a), (c) and (e)). A slight reduction in $MI_{LoG\text{-}LowFreq}$ was found in the contralateral slm layer during CCAO occlusion (Figure 7(b) and (f)).

The main effects of dMCAO or CCAO on brain oscillations over time periods during acute ischemia are summarized in Supplementary Table 1. Persistent reduction of theta-gamma modulation is consistent with the reduction of T/D ratio during the same period of time. Because LTD occurrence was increased during the occlusion period, the analysis was also extended to LTD. However, there was no significant change in the above parameters compared to baseline during LTD period of dMCAO animals (Supplementary Table 2). Neither stroke nor mild ischemia induced significant changes in delta or gamma oscillations in the intact ipsilateral cortex distal to ischemic lesion, or in the homotopic contralateral side (Supplementary Figure 1). The main effects of dMCAO or CCAO over time periods on delta and gamma power are summarized in Supplementary Table 3.

Discussion

While the effect of reduced CBF on scalp EEG has been well documented in humans, the specific oscillatory activity changes in deeper brain regions remote from the stroke lesion site still remain poorly understood. With extracellular multi-site electrophysiology recordings conducted under urethane anesthesia, we detected temporary decreases in the power of theta and gamma oscillations following dMCAO but not CCAO, which were likely attributable to a quick recovery of CBF in the latter due to robust collateral compensation. A reduction in the high theta brain state was observed after both dMCAO and CCAO, although a significant and persistent reduction of T/D amplitude ratio was only found after dMCAO. Furthermore, dMCAO but

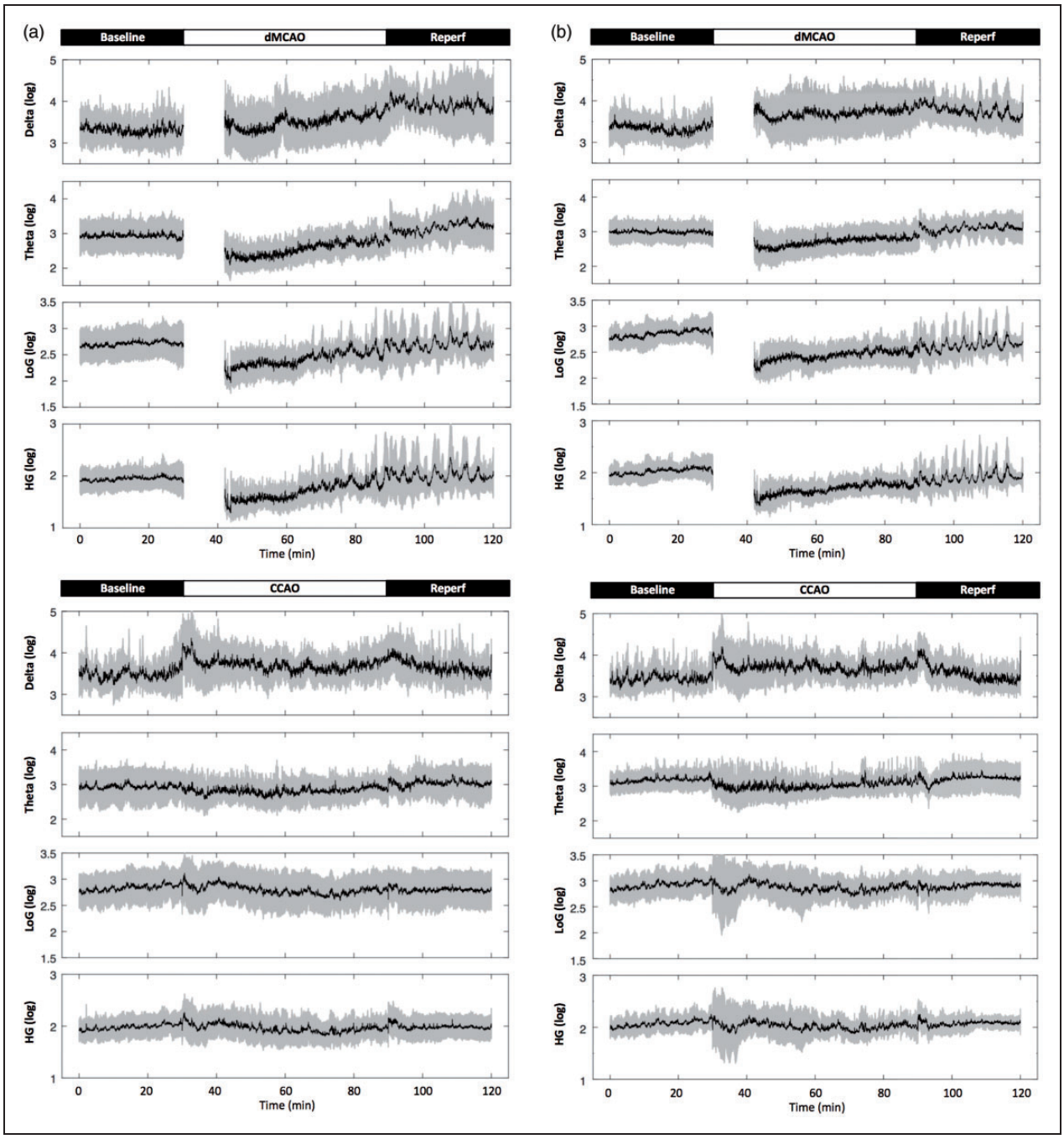

Figure 4. Cortical stroke induces temporary reduction in the power of theta and gamma oscillation in the hippocampal slm. (a and b), representative 2-h time series for the parameters as indicated in rats subjected to temporary cortical stroke (dMCAO) or mild ischemia (CCAO) for ipsilateral (a) and contralateral (b) recordings in the slm. Data are expressed in logarithm scale. Black lines and gray shades represent mean and SD, respectively. (c and d), Quantification of temporal changes in hippocampal oscillatory activity in ipsilateral (upper open bar panels) (c) and contralateral hippocampus (lower solid bar panels) (d). The continuous data for each variable were grouped into four time periods as baseline (0–30 min), 1st occlusion (30–60 min), 2nd occlusion (60–90 min) and reperfusion (90–120 min). One-way analysis of variance (ANOVA) for the time periods was used to determine changes induced by CCAO (blue) or dMCAO. Data for the 1st occlusion period in the dMCAO group were only partially plotted or excluded for statistics due to a procedural delay. A follow-up post hoc analysis was performed to reveal a detailed temporal profile for each variable if necessary. Theta and low gamma (LoG) power was reduced in the bilateral stratum lacunosum moleculare during dMCAO occlusion compared to baseline, while high gamma (HiG) power was reduced contralaterally. Unlike dMCAO, mild ischemia via CCAO did not induce significant changes in theta or gamma oscillations compared to baseline. The time series plots show greater dynamic changes of power in all frequencies during dMCAO reperfusion not revealed by the averages of power during the time period $^{*}p < 0.05$, $^{**}p < 0.01$, $^{***}p < 0.001$. dMCAO: N = 10; CCAO: N = 7.

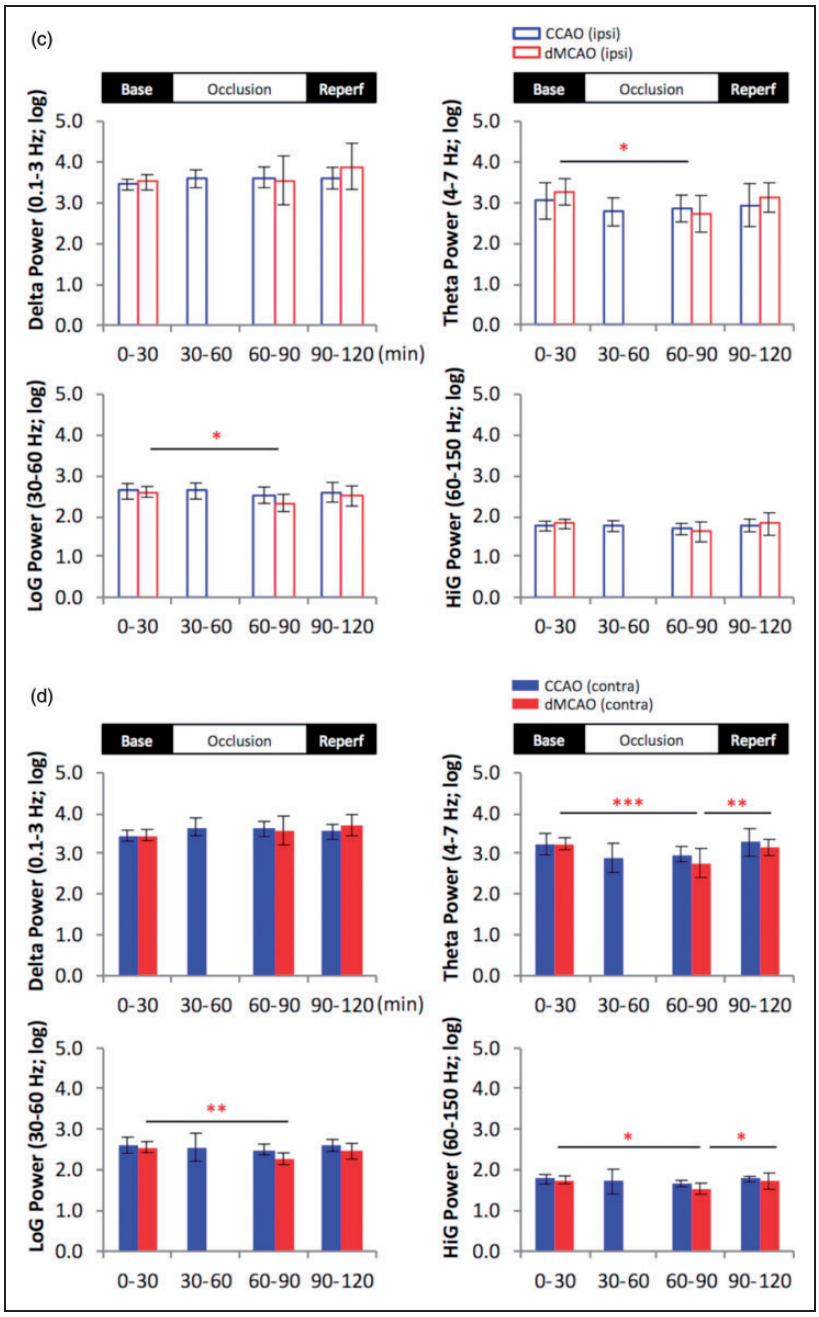

Figure 4. Continued.

not CCAO induced an increased occurrence of the SWRs and HFDs during ischemic reperfusion period, suggesting that cortical stroke affected the interplay between excitatory and inhibitory circuit in the hippocampus. The more pronounced changes in hippocampal oscillations following the dMCAO likely reflect permanent neuronal loss in the cortex that resulted in the disruption of brain connectivity between the cortex and hippocampus or other limbic regions, as evidenced by the change in phase-amplitude coupling between hippocampal theta and cortical gamma oscillations.

Imaging-based connectivity data show that stroke in humans leads to network disturbance not only in the vicinity of the brain lesion but also between remote cortical areas in bilateral hemispheres.[59,60] Brain regions in the entorhinal cortex, perirhinal cortex and the temporal lobe are reciprocally connected with the dMCAO lesioned regions in the rats, suggesting that experimental stroke may alter the input from the damaged regions to the lateral entorhinal cortex, and/or by changing the synaptic activity among the remaining intact regions including the hippocampus.

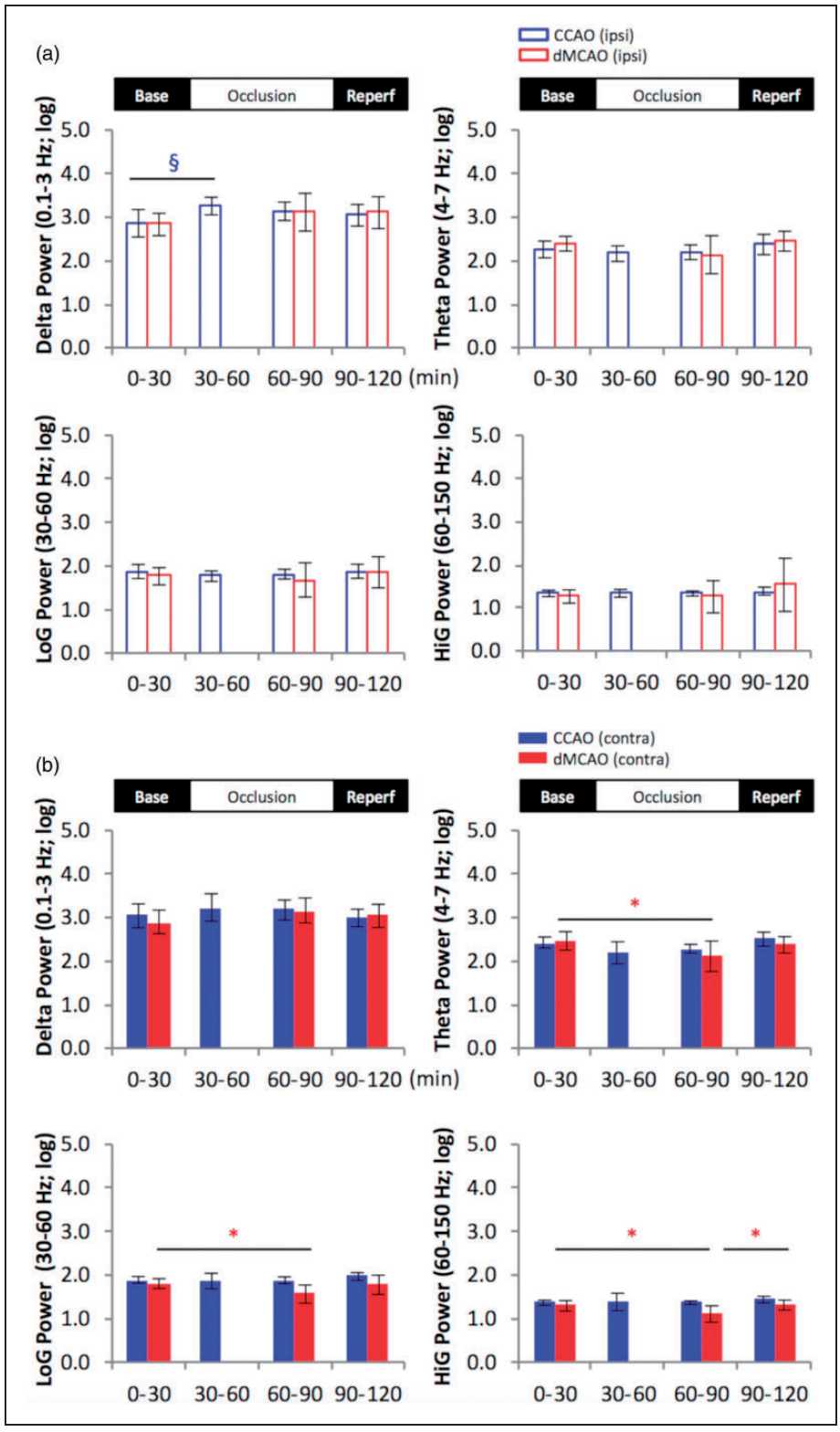

Figure 5. Stroke reduces theta and gamma power in the contralateral CA1 pyramidal layer. Comparison of temporal changes in hippocampal oscillatory power in the ipsilateral (A: upper open bar panel) and contralateral hemisphere (B: lower solid bar panel). Multiple comparisons between baseline and the other time periods revealed that dMCAO reduced theta, low- and high-gamma power in the contralateral hemisphere during occlusion compared to baseline period, while CCAO transiently increased delta power during the first 30-min period of occlusion in the ipsilateral CA1 pyramidal layer. $^{*}p < 0.05$ (for dMCAO); $^{\S}p < 0.05$ (for CCAO): $p < 0.05$. dMCAO: N = 10; CCAO: N = 7.

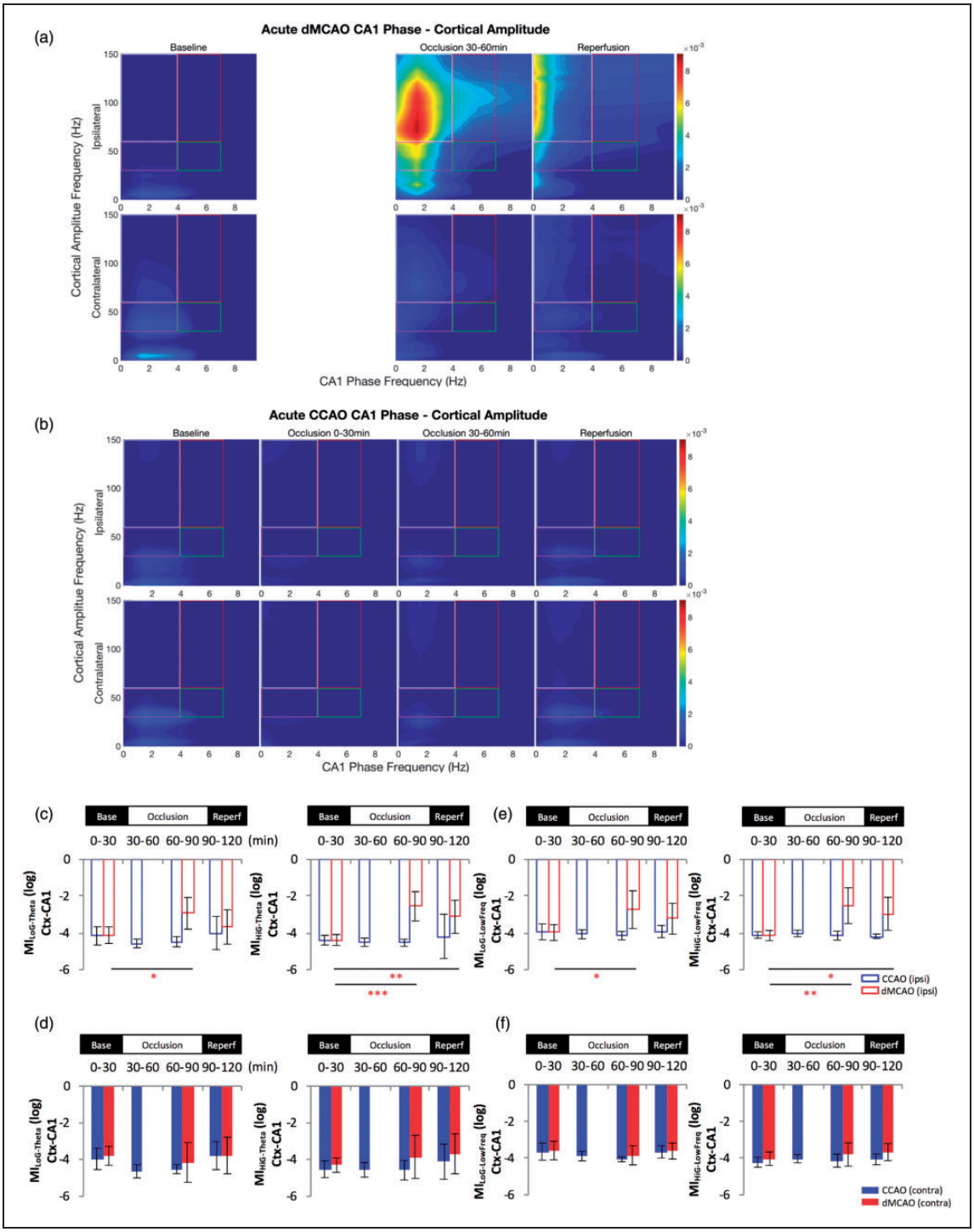

Figure 6. Cortical gamma power is modulated by hippocampal low frequency phase in the CA1 following cortical stroke. Comparison of temporal modulation of cortical gamma amplitude by theta phase (4–7 Hz) (a–d) and low frequency (0–4 Hz) phase (e–f) in the CA1 of the ipsilateral (open bar panels) and contralateral hemisphere (solid bar panels) revealed an increase of the theta-gamma and low frequency wave-gamma modulation index in the ipsilateral hemisphere during acute dMCAO. Cross frequency coupling was confirmed by the phase-amplitude comodulogram computed for LFP signals from baseline (left), during occlusion (one to two middle panels) and after reperfusion (right) in the ipsilateral and contralateral hemisphere following dMCAO (a) and CCAO (b) within the grids as indicated. The CA1 theta phase and low-frequency wave phase modulation of the cortical layer gamma oscillations was increased for both low and high gamma bands, respectively. The increase of $MI_{HiG\text{-}Theta}$ and $Mi_{HiG\text{-}Low\ Freq}$ also extended to the reperfusion phase of dMCAO (c, e). CCAO did not lead to significant changes of MI of either gamma bands. $^{*}p < 0.05$, $^{**}p < 0.01$, $^{***}p < 0.001$ (for dMCAO) for multiple comparisons between baseline and other levels. dMCAO: N = 10; CCAO: N = 7.

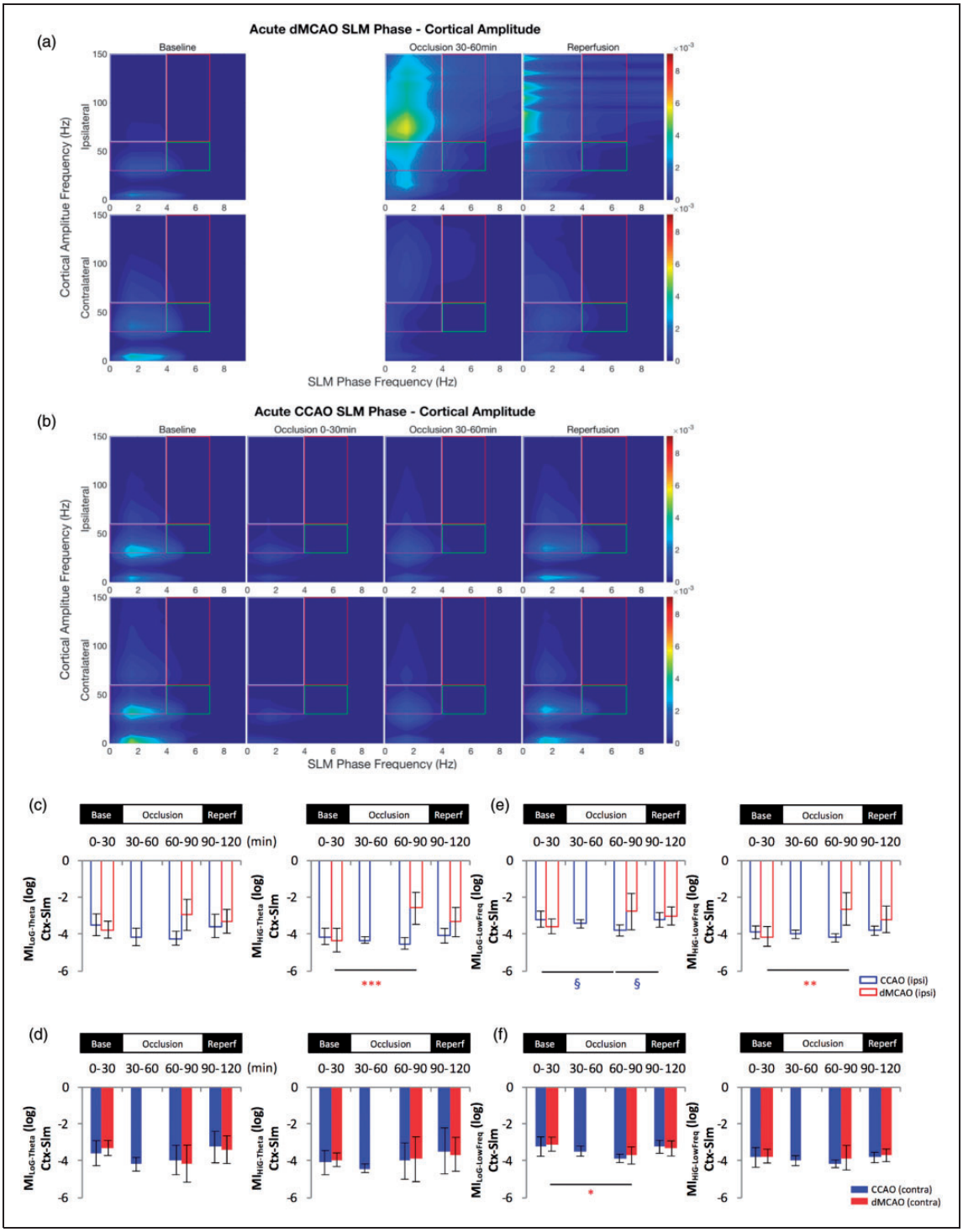

Figure 7. Cortical gamma power is modulated by hippocampal low frequency phase in the slm following cortical stroke. Comparison of temporal modulation of cortical gamma amplitude by low frequencies oscillations phase in the slm layer of the ipsilateral and contralateral hemisphere revealed an increase of the theta-high gamma modulation index (a–d) and an increase of the coupling between high gamma and lower frequencies (0–4 Hz) (e–f) in the ipsilateral hemisphere during acute dMCAO. The phase-amplitude comodulogram (a–b) confirmed the coupling between theta or low frequencies and high oscillations observed in the bar graph representations (c–f) in the ipsilateral hemisphere during MCA occlusion. In contrast, little change in theta-gamma modulation or lower frequencies coupling was observed following CCAO except for a brief decrease of $Mi_{HiG\text{-}Theta}$ (c) and $Mi_{LoG\text{-}Low\ Freq}$ (e) during the CCA occlusion in the slm layer of the ipsilateral side. $^{*}p < 0.05$, $^{**}p < 0.01$, (for dMCAO); $^{\S}p < 0.05$ (for CCAO) for multiple comparisons between baseline and other levels. dMCAO: N = 10; CCAO: N = 7.

Our recent connectome analysis at the mesoscale confirmed that dMCAO reduced the reciprocal connections of the remaining intact brain regions involved in spatial information processing,[11] which could lead to altered connectivity and functional activation among these regions. Some of the perturbation of brain connectivity reported after stroke could be attributed to altered excitotary and inhibitory drives. For example, $GABA_aR$ downregulation is observed after stroke both pre- and post-synaptically in ischemic area,[61] while in vitro blockade of $GABA_aR$ increases the excitability of infarcted slices after ischemia.[62] In addition, $GABA_aR$ and $GABA_bR$ are downregulated after hippocampal ischemia in guinea pig[63] and after focal ischemia in mice,[9] respectively. Because a long-term disruption of cortico-hippocampal networks is necessary for cognitive decline, one limitation of the current study is the lack of brain oscillation data during chronic stroke. A thorough investigation in relevant electrophysiological signature in rats with chronic stroke is underway[64] and would be insightful to understand the long-term adaptation of brain recovering from acute ischemic brain injury.

Because the generation and regulation of ripple firing appears to depend on the precise interplay between excitatory pyramidal neurons and inhibitory interneurons,[65–67] the aberrant ripple occurrence observed in our stroke model is likely due to altered excitatory and inhibitory networks in the hippocampus caused by the ischemia-induced deafferentation. Consistent with this notion, augmented ripple oscillations were found in mutant mice with reduced AMPA receptor in PV(+) interneurons.[16] However, the neuronal populations participating in the regulation of physiological ripple oscillations and their phenotypes are complex, requiring orchestrated actions of synchronous activation of excitatory pyramidal cells and certain classes of inhibitory GABAergic interneurons.[68–70] Focal pharmacological blockade of $GABA_A$ receptors abolished ripples,[18] while an antagonist of a $GABA_AR5$ enhanced the power and duration of the SWRs.[62,67] Apart from the acute disturbance of excitatory and inhibitory circuits as observed in the current stroke study, a number of mouse models of neurodegeneration with altered hippocampal inhibitory drive also displayed changes in the SWR. For example, diminished ripple occurrence rate was found in aged mice with human Apolipoprotein E4 knocked in[71] that led to the loss of hilar GABAergic interneurons,[72] while rTg4510 transgenic mice, a model of tauopathy and dementia, had reduced inhibitory control of hippocampal network and smaller amplitude-SWRs.[73]

Similar to our observation, mice undergoing unilateral photothrombosis in the hippocampus also displayed bilateral HFDs.[51] Unlike the dMCAO stroke that did not produce hippocampal injury, unilateral hippocampal photothrombotic stroke induced extensive hippocampal infarction and elicited an immediate DC voltage shift and reduced gamma activity ipsilaterally. However, some HFDs recorded in the hippocampal photothrombotic model in the range of 250–450 Hz and reminiscent of epileptiform dischages were also detected in our dMCAO model. Consistent with the notion that aberrant or pathological ripples are implicated in neurological diseases and functional deficits,[74] high amplitude SWRs were reported in epilepsy patients.[75]

It is well established that CBF reduction induces EEG abnormality due to energy deprivation-induced changes in the membrane potential of neurons.[13,14] Progressive loss of fast frequency rhythms and increase in low frequency ones such as the delta wave is often observed with increasing degree of brain ischemia in the ipsilateral cortical regions. Gamma oscillations in the hippocampus are particularly sensitive to decreases in pO_2.[76] The impairment in functional activation and aberrant hippocampal oscillations could also be caused by below-infarct-threshold level of CBF reduction that goes far beyond the ischemic core, as supported by a recent study showing that the disruption of neural activity in the barrel cortex surrounding photothrombotic microinfarcts appeared to be inversely correlated with the distance from the infarct border, resulting in a greater volume of neural deficits compared to the volume of infarct core by 12 folds.[77]

Hippocampal theta rhythm has been implicated in the coding of information and coordination of cellular processes related to memory.[21,78–80] Apart from cognitive processes, the frequency and power of the hippocampal theta vary with behavior and were reportedly affected by movement speed,[81,82] visual novelty[83] and nasal respiration.[84] Increased hippocampal theta amplitude was detected even under urethane anesthesia following the treatment of cognition-enhancing drugs.[85] However, the change in hippocampal theta power recorded under anesthesia following brain ischemia detected in our study is unlikely to be related to changes in behavior as observed in the awake state. Instead, it is more likely that the brain is transitioning into the energy saving mode of slower oscillations after ischemia due to reduced oxygen metabolism, coinciding with a concurrent reduction in the amplitude of gamma oscillations. Stroke-induced reduction in the amplitudes of multiple frequency bands appears to persist until at least one month after stroke (unpublished observation), implicating a long-lasting effect of ischemic injury on the disruption of brain activity. Similar to ischemic stroke, traumatic brain injury that produced cognitive

impairment was also associated with reduced hippocampal theta amplitude and frequency.[86]

Interaction between oscillations in different frequencies can occur via phase-amplitude coupling, resulting in synchronization of amplitude envelope of faster rhythms within the phase of slower rhythms. Phase-amplitude coupling is universally observed in several brain regions including the hippocampus, basal ganglia and neocortex of many species.[53] Recently, the theta phase modulation of gamma amplitude during place cell firing has received great attention, and has been causally linked to spatial navigation and cognitive performances in rodents.[87–89] Unexpectedly, we found that the coupling between cortical gamma power and hippocampal theta as well as low frequency oscillations was increased during dMCAO occlusion and persisted after reperfusion. Interestingly, increased modulation of low gamma power was reported in the near death state of Wistar rats, although by alpha- (10–15 Hz) and theta oscillations (5–10 Hz),[90] providing a frame work to explain the lucid consciousness experienced during near death. On the other hand, the increased MI detected in our stroke model may reflect an attempt to compensate for the loss of connectivity between the cortex and hippocampus during ischemia, although the state of cognitive processing or consciousness of these stroke rats remains unknown. Consistent with previous data, the slow wave phase that modulates the gamma power in our study is likely to be related to anesthesia.[90] In addition, another recent study found that a near-theta and respiration-entrained rhythm (>1 Hz) was coupled to the 80–120 Hz gamma band in several brain regions of freely moving mice,[91] suggesting that gamma can be modulated by a variety of slow oscillations relevant to the physiological states during cross frequency coupling.

The main impediment curbing the translation of our findings stems from the recording condition, since general anesthetics are known to reduce spike activity.[92] Nonetheless, urethane is considered a good choice of anesthetic for physiological studies due to its modest effect on neuronal activity, e.g. it causes a small potentiation of GABA and glycine inhibition as well as a small reduction in glutamate excitation in the brain compared to other more selective anesthetics.[93] Moreover, urethane anesthesia not only preserves all the brain rhythms investigated in our study, but also induces spontaneous and rhythmic brain state alternations mimicking the natural sleep in mice and rats.[92,94] In fact, most of our earlier knowledge in cell type-specific brain oscillations in the hippocampus came from studies using urethane anesthesia.[65] Due to its minimal effects on autonomic and cardiovascular systems and long-lasting anesthetic effect,[95] it offers a stable and reproducible platform for our experimental paradigm. Furthermore, it is well established that hippocampal theta rhythm recorded under urethane[96] is comparable to awake recording.[97] A recent optogenetic study also confirms that septal cholinergic input generates hippocampal theta in both awake and anesthetized conditions,[98] further affirming that urethane anesthesia is appropriate for studying network activity involving the hippocampus. Lastly, urethane anesthesia has been successfully used in the stroke community to study patterns of intracortical LFPs as a diagnostic for epileptiform discharge,[99] as well as other oscillatory changes,[13,14] and it led to a similar infarct size as halothane anesthesia.[100] Despite the effect of anesthesia on neuronal activity, many electrophysiological changes detected in our study are specific to MCA stroke, since they are not present during baseline nor following CCAO that were also recorded under the same condition of anesthesia.

Apart from stroke diagnosis and monitoring the efficacy of thrombolysis, a number of electrophysiological correlates have also been used to predict post stroke disability and recovery.[13] For example, an aberrant interhemispheric asynchrony measured by EEG is a useful predictor for post-stroke disability that outperforms conventional methods of focusing on delta oscillations,[101–103] although the overreliance on interhemispheric balancing as indices for recovery has been challenged.[104] However, electrophysiological correlates for cognitive recovery are not well established. For example, the reliability of P300 wave, a large EEG positivity that peaked around 300 ms after the stimulus appeared, in assessing post stroke cognitive processes such as attention and memory has not been proven,[105,106] due to wide influence on P300 by biological and environmental factors.[107] It is also suggested that the P300 may not be suitable for all stroke subtypes, especially MCA stroke, nor for chronic stroke. To the contrary, the aberrant change of hippocampal oscillations in the current study may be a useful biomarker for post stroke cognitive function if properly validated in awake rats performing behavioral tasks during chronic stroke, as some variables have been proposed as the potential neural substrates of cognitive impairment in brain disease.[108,109]

Funding

The author(s) disclosed receipt of the following financial support for the research, authorship, and/or publication of this article: This work was supported by NIH grant R01 NS102886 (JL), VA merit award I01BX003335, Research Career Scientist award IK6BX004600 (JL), the Eunice Kennedy Shiver National Institute of Child Health & Human Development of the National Institutes of Health under Award Number K12HD073945 (AY), and the Center for Neurotechnology (CNT, a National Science

Foundation Engineering Research Center under Grant EEC-1028725) (AY).

Declaration of conflicting interests

The author(s) declared no potential conflicts of interest with respect to the research, authorship, and/or publication of this article.

Authors' contributions

Ji-Wei He: performed the recording and analysis, and contributed to manuscript writing.
Gratianne Rabiller: performed the recording and analysis, and contributed to manuscript writing.
Yasuo Nishijima: performed the dMCAO CCAO surgery.
Yosuke Akamatsu: performed the dMCAO CCAO surgery.
Karam Khateeb: performed a part of the data analysis.
Azadeh Yazdan-Shahmorad: performed some data analysis and contributed to the overall manuscript editing.
Jialing Liu: provided the overal idea, design, logistics and writing of the manuscript.

Supplemental material

Supplemental material for this paper can be found at the journal website: http://journals.sagepub.com/home/jcb

References

1. Khedr EM, Hamed SA, El-Shereef HK, et al. Cognitive impairment after cerebrovascular stroke: relationship to vascular risk factors. *Neuropsychiatr Dis Treat* 2009; 5: 103–116.
2. Barker-Collo SL, Feigin VL, Lawes CM, et al. Attention deficits after incident stroke in the acute period: frequency across types of attention and relationships to patient characteristics and functional outcomes. *Top Stroke Rehabil* 2010; 17: 463–476.
3. Cumming TB, Plummer-D'Amato P, Linden T, et al. Hemispatial neglect and rehabilitation in acute stroke. *Arch Phys Med Rehabil* 2009; 90: 1931–1936.
4. Bederson JB, Pitts LH, Tsuji M, et al. Rat middle cerebral artery occlusion: evaluation of the model and development of a neurologic examination. *Stroke* 1986; 17: 472–476.
5. Iizuka H, Sakatani K and Young W. Selective cortical neuronal damage after middle cerebral artery occlusion in rats. *Stroke* 1989; 20: 1516–1523.
6. Liu F and McCullough LD. Middle cerebral artery occlusion model in rodents: methods and potential pitfalls. *J Biomed Biotechnol* 2011; 2011: 464701.
7. Okada M, Nakanishi H, Tamura A, et al. Long-term spatial cognitive impairment after middle cerebral artery occlusion in rats: no involvement of the hippocampus. *J Cereb Blood Flow Metab* 1995; 15: 1012–1021.
8. Wang Y, Bontempi B, Lesburguere E, et al. Environmental enrichment preserves cortical inputs to the parahippocampal areas and reduces post stroke diaschisis. *Am J Neuroprotect Neuroregenerat* 2011; 3: 66–76.
9. Kim JY, Ho H, Kim N, et al. Calcium-sensing receptor (CaSR) as a novel target for ischemic neuroprotection. *Ann Clin Transl Neurol* 2014; 1: 851–866.
10. Mayor D and Tymianski M. Neurotransmitters in the mediation of cerebral ischemic injury. *Neuropharmacology* 2018; 134(Pt B): 178–188.
11. Schmitt O, Badurek S, Liu W, et al. Prediction of regional functional impairment following experimental stroke via connectome analysis. *Sci Rep* 2017; 7: 46316.
12. Silasi G and Murphy TH. Stroke and the connectome: how connectivity guides therapeutic intervention. *Neuron* 2014; 83: 1354–1368.
13. Rabiller G, He JW, Nishijima Y, et al. Perturbation of brain oscillations after ischemic stroke: a potential biomarker for post-stroke function and therapy. *Int J Mol Sci* 2015; 16: 25605–25640.
14. Moyanova SG and Dijkhuizen RM. Present status and future challenges of electroencephalography- and magnetic resonance imaging-based monitoring in preclinical models of focal cerebral ischemia. *Brain Res Bull* 2014; 102: 22–36.
15. Buzsaki G. Hippocampal sharp wave-ripple: a cognitive biomarker for episodic memory and planning. *Hippocampus* 2015; 25: 1073–1188.
16. Racz A, Ponomarenko AA, Fuchs EC, et al. Augmented hippocampal ripple oscillations in mice with reduced fast excitation onto parvalbumin-positive cells. *J Neurosci* 2009; 29: 2563–2568.
17. Schlingloff D, Kali S, Freund TF, et al. Mechanisms of sharp wave initiation and ripple generation. *J Neurosci* 2014; 34: 11385–11398.
18. Stark E, Roux L, Eichler R, et al. Pyramidal cell-interneuron interactions underlie hippocampal ripple oscillations. *Neuron* 2014; 83: 467–480.
19. Jadhav SP, Kemere C, German PW, et al. Awake hippocampal sharp-wave ripples support spatial memory. *Science* 2012; 336: 1454–1458.
20. Carr MF, Jadhav SP and Frank LM. Hippocampal replay in the awake state: a potential substrate for memory consolidation and retrieval. *Nat Neurosci* 2011; 14: 147–153.
21. Buzsaki G. Theta oscillations in the hippocampus. *Neuron* 2002; 33: 325–340.
22. Battaglia FP, Benchenane K, Sirota A, et al. The hippocampus: hub of brain network communication for memory. *Trends Cogn Sci* 2011; 15: 310–318.
23. Ognjanovski N, Maruyama D, Lashner N, et al. CA1 hippocampal network activity changes during sleep-dependent memory consolidation. *Front Syst Neurosci* 2014; 8: 61.
24. Mitra A, Snyder AZ, Hacker CD, et al. Human cortical-hippocampal dialogue in wake and slow-wave sleep. *Proc Natl Acad Sci U S A* 2016; 113: E6868–E6876.
25. McNaughton N, Ruan M and Woodnorth MA. Restoring theta-like rhythmicity in rats restores initial learning in the Morris water maze. *Hippocampus* 2006; 16: 1102–1110.
26. Shirvalkar PR, Rapp PR and Shapiro ML. Bidirectional changes to hippocampal theta-gamma comodulation predict memory for recent spatial episodes. *Proc Natl Acad Sci U S A* 2010; 107: 7054–7059.

27. Gray CM. Synchronous oscillations in neuronal systems: mechanisms and functions. *J Comput Neurosci* 1994; 1: 11–38.
28. Cirelli C and Tononi G. Cortical development, electroencephalogram rhythms, and the sleep/wake cycle. *Biol Psychiatry* 2015; 77: 1071–1078.
29. Fell J, Fernandez G, Klaver P, et al. Rhinal-hippocampal coupling during declarative memory formation: dependence on item characteristics. *Neurosci Lett* 2006; 407: 37–41.
30. Fries P, Reynolds JH, Rorie AE, et al. Modulation of oscillatory neuronal synchronization by selective visual attention. *Science* 2001; 291: 1560–1563.
31. Wang XJ. Neurophysiological and computational principles of cortical rhythms in cognition. *Physiol Rev* 2010; 90: 1195–1268.
32. Buzsaki G and Wang XJ. Mechanisms of gamma oscillations. *Ann Rev Neurosci* 2012; 35: 203–225.
33. Trimper JB, Galloway CR, Jones AC, et al. Gamma oscillations in rat hippocampal subregions dentate gyrus, CA3, CA1, and subiculum underlie associative memory encoding. *Cell Rep* 2017; 21: 2419–2432.
34. Bragin A, Jando G, Nadasdy Z, et al. Gamma (40-100 Hz) oscillation in the hippocampus of the behaving rat. *J Neurosci* 1995; 15: 47–60.
35. Hanslmayr S, Staresina BP and Bowman H. Oscillations and episodic memory: addressing the synchronization/desynchronization conundrum. *Trends Neurosci* 2016; 39: 16–25.
36. Heusser AC, Poeppel D, Ezzyat Y, et al. Episodic sequence memory is supported by a theta-gamma phase code. *Nat Neurosci* 2016; 19: 1374–1380.
37. Montgomery SM and Buzsaki G. Gamma oscillations dynamically couple hippocampal CA3 and CA1 regions during memory task performance. *Proc Natl Acad Sci U S A* 2007; 104: 14495–14500.
38. Carr MF, Karlsson MP and Frank LM. Transient slow gamma synchrony underlies hippocampal memory replay. *Neuron* 2012; 75: 700–713.
39. Zhang X, Zhong W, Brankack J, et al. Impaired theta-gamma coupling in APP-deficient mice. *Sci Rep* 2016; 6: 21948.
40. Barr MS, Rajji TK, Zomorrodi R, et al. Impaired theta-gamma coupling during working memory performance in schizophrenia. *Schizophr Res* 2017; 189: 104–110.
41. Astrup J, Siesjo BK and Symon L. Thresholds in cerebral ischemia – the ischemic penumbra. *Stroke* 1981; 12: 723–725.
42. Alia C, Spalletti C, Lai S, et al. Reducing GABAA-mediated inhibition improves forelimb motor function after focal cortical stroke in mice. *Sci Rep* 2016; 6: 37823.
43. Balbinot G and Schuch CP. Compensatory relearning following stroke: cellular and plasticity mechanisms in rodents. *Front Neurosci* 2018; 12: 1023.
44. Sun H, Le T, Chang TT, et al. AAV-mediated netrin-1 overexpression increases peri-infarct blood vessel density and improves motor function recovery after experimental stroke. *Neurobiol Dis* 2011; 44: 73–83.
45. Leinekugel X, Khazipov R, Cannon R, et al. Correlated bursts of activity in the neonatal hippocampus in vivo. *Science* 2002; 296: 2049–2052.
46. Sun C, Sun H, Wu S, et al. Conditional ablation of neuroprogenitor cells in adult mice impedes recovery of post-stroke cognitive function and reduces synaptic connectivity in the perforant pathway. *J Neurosci* 2013; 33: 17314–17325.
47. Scheffer-Teixeira R, Belchior H, Caixeta FV, et al. Theta phase modulates multiple layer-specific oscillations in the CA1 region. *Cereb Cortex* 2012; 22: 2404–2414.
48. Shinohara Y, Hosoya A and Hirase H. Experience enhances gamma oscillations and interhemispheric asymmetry in the hippocampus. *Nat Commun* 2013; 4: 1652.
49. Lockmann AL, Laplagne DA, Leao RN, et al. A respiration-coupled rhythm in the rat hippocampus independent of theta and slow oscillations. *J Neurosci* 2016; 36: 5338–5352.
50. Wolansky T, Clement EA, Peters SR, et al. Hippocampal slow oscillation: a novel EEG state and its coordination with ongoing neocortical activity. *J Neurosci* 2006; 26: 6213–6229.
51. Barth AM and Mody I. Changes in hippocampal neuronal activity during and after unilateral selective hippocampal ischemia in vivo. *J Neurosci* 2011; 31: 851–860.
52. Karlsson MP and Frank LM. Awake replay of remote experiences in the hippocampus. *Nat Neurosci* 2009; 12: 913–918.
53. Tort AB, Komorowski R, Eichenbaum H, et al. Measuring phase-amplitude coupling between neuronal oscillations of different frequencies. *J Neurophysiol* 2010; 104: 1195–1210.
54. Williams AJ, Lu XC, Hartings JA, et al. Neuroprotection assessment by topographic electroencephalographic analysis: effects of a sodium channel blocker to reduce polymorphic delta activity following ischaemic brain injury in rats. *Fundam Clin Pharmacol* 2003; 17: 581–593.
55. Williams AJ and Tortella FC. Neuroprotective effects of the sodium channel blocker RS100642 and attenuation of ischemia-induced brain seizures in the rat. *Brain Res* 2002; 932: 45–55.
56. Aminov A, Rogers JM, Johnstone SJ, et al. Acute single channel EEG predictors of cognitive function after stroke. *PLoS One* 2017; 12: e0185841.
57. Jordan KG. Emergency EEG and continuous EEG monitoring in acute ischemic stroke. *J Clin Neurophysiol* 2004; 21: 341–352.
58. Nishijima Y, Akamatsu Y, Yang SY, et al. Impaired collateral flow compensation during chronic cerebral hypoperfusion in the type 2 diabetic mice. *Stroke* 2016; 47: 3014–3021.
59. Duering M, Righart R, Wollenweber FA, et al. Acute infarcts cause focal thinning in remote cortex via degeneration of connecting fiber tracts. *Neurology* 2015; 84: 1685–1692.
60. Kuchcinski G, Munsch F, Lopes R, et al. Thalamic alterations remote to infarct appear as focal iron accumulation and impact clinical outcome. *Brain* 2017; 140: 1932–1946.

61. Schwartz-Bloom RD and Sah R. gamma-Aminobutyric acid(A) neurotransmission and cerebral ischemia. *J Neurochem* 2001; 77: 353–371.
62. Atack JR, Bayley PJ, Seabrook GR, et al. L-655,708 enhances cognition in rats but is not proconvulsant at a dose selective for alpha5-containing GABAA receptors. *Neuropharmacology* 2006; 51: 1023–1029.
63. Miller SM, Sullivan SM, Ireland Z, et al. Neonatal seizures are associated with redistribution and loss of GABAA alpha-subunits in the hypoxic-ischaemic pig. *J Neurochem* 2016; 139: 471–484.
64. Ip Z, Rabiller G, He JW, et al. Cortical stroke affects activity and stability of theta/delta states in remote hippocampal regions. In: *41st Annual IEEE Eng Med Biol Conf*, Berlin, Germany, 23–27 July 2019.
65. Klausberger T and Somogyi P. Neuronal diversity and temporal dynamics: the unity of hippocampal circuit operations. *Science* 2008; 321: 53–57.
66. Ellender TJ, Nissen W, Colgin LL, et al. Priming of hippocampal population bursts by individual perisomatic-targeting interneurons. *J Neurosci* 2010; 30: 5979–5991.
67. Papatheodoropoulos C and Koniaris E. alpha5GABAA receptors regulate hippocampal sharp wave-ripple activity in vitro. *Neuropharmacology* 2011; 60: 662–673.
68. Ylinen A, Bragin A, Nadasdy Z, et al. Sharp wave-associated high-frequency oscillation (200 Hz) in the intact hippocampus: network and intracellular mechanisms. *J Neurosci* 1995; 15: 30–46.
69. Csicsvari J, Hirase H, Czurko A, et al. Fast network oscillations in the hippocampal CA1 region of the behaving rat. *J Neurosci* 1999; 19: RC20.
70. Klausberger T, Magill PJ, Marton LF, et al. Brain-state- and cell-type-specific firing of hippocampal interneurons in vivo. *Nature* 2003; 421: 844–848.
71. Gillespie AK, Jones EA, Lin YH, et al. Apolipoprotein E4 Causes age-dependent disruption of slow gamma oscillations during hippocampal sharp-wave ripples. *Neuron* 2016; 90: 740–751.
72. Andrews-Zwilling Y, Bien-Ly N, Xu Q, et al. Apolipoprotein E4 causes age- and tau-dependent impairment of GABAergic interneurons, leading to learning and memory deficits in mice. *J Neurosci* 2010; 30: 13707–13717.
73. Witton J, Staniaszek LE, Bartsch U, et al. Disrupted hippocampal sharp-wave ripple-associated spike dynamics in a transgenic mouse model of dementia. *J Physiol* 2016; 594: 4615–4630.
74. van Diessen E, Hanemaaijer JI, Otte WM, et al. Are high frequency oscillations associated with altered network topology in partial epilepsy? *Neuroimage* 2013; 82: 564–573.
75. Pail M, Rehulka P, Cimbalnik J, et al. Frequency-independent characteristics of high-frequency oscillations in epileptic and non-epileptic regions. *Clin Neurophysiol* 2017; 128: 106–114.
76. Huchzermeyer C, Albus K, Gabriel HJ, et al. Gamma oscillations and spontaneous network activity in the hippocampus are highly sensitive to decreases in pO2 and concomitant changes in mitochondrial redox state. *J Neurosci* 2008; 28: 1153–1162.
77. Summers PM, Hartmann DA, Hui ES, et al. Functional deficits induced by cortical microinfarcts. *J Cereb Blood Flow Metab* 2017; 37: 3599–3614.
78. Hasselmo ME. What is the function of hippocampal theta rhythm? Linking behavioral data to phasic properties of field potential and unit recording data. *Hippocampus* 2005; 15: 936–949.
79. Buzsaki G. Theta rhythm of navigation: link between path integration and landmark navigation, episodic and semantic memory. *Hippocampus* 2005; 15: 827–840.
80. Vertes RP. Hippocampal theta rhythm: a tag for short-term memory. *Hippocampus* 2005; 15: 923–935.
81. Whishaw IQ and Vanderwolf CH. Hippocampal EEG and behavior: changes in amplitude and frequency of RSA (theta rhythm) associated with spontaneous and learned movement patterns in rats and cats. *Behav Biol* 1973; 8: 461–484.
82. Slawinska U and Kasicki S. The frequency of rat's hippocampal theta rhythm is related to the speed of locomotion. *Brain Res* 1998; 796: 327–331.
83. Jeewajee A, Lever C, Burton S, et al. Environmental novelty is signaled by reduction of the hippocampal theta frequency. *Hippocampus* 2008; 18: 340–348.
84. Yanovsky Y, Ciatipis M, Draguhn A, et al. Slow oscillations in the mouse hippocampus entrained by nasal respiration. *J Neurosci* 2014; 34: 5949–5964.
85. Kinney GG, Patino P, Mermet-Bouvier Y, et al. Cognition-enhancing drugs increase stimulated hippocampal theta rhythm amplitude in the urethane-anesthetized rat. *J Pharmacol Exp Ther* 1999; 291: 99–106.
86. Fedor M, Berman RF, Muizelaar JP, et al. Hippocampal theta dysfunction after lateral fluid percussion injury. *J Neurotrauma* 2010; 27: 1605–1615.
87. Tort AB, Komorowski RW, Manns JR, et al. Theta-gamma coupling increases during the learning of item-context associations. *Proc Natl Acad Sci U S A* 2009; 106: 20942–20947.
88. Siegle JH and Wilson MA. Enhancement of encoding and retrieval functions through theta phase-specific manipulation of hippocampus. *Elife* 2014; 3: e03061.
89. O'Keefe J and Recce ML. Phase relationship between hippocampal place units and the EEG theta rhythm. *Hippocampus* 1993; 3: 317–330.
90. Borjigin J, Lee U, Liu T, et al. Surge of neurophysiological coherence and connectivity in the dying brain. *Proc Natl Acad Sci U S A* 2013; 110: 14432–14437.
91. Zhong W, Ciatipis M, Wolfenstetter T, et al. Selective entrainment of gamma subbands by different slow network oscillations. *Proc Natl Acad Sci U S A* 2017; 114: 4519–4524.
92. Suzuki SS and Smith GK. Spontaneous EEG spikes in the normal hippocampus. V. Effects of ether, urethane, pentobarbital, atropine, diazepam and bicuculline. *Electroencephalogr Clin Neurophysiol* 1988; 70: 84–95.
93. Hara K and Harris RA. The anesthetic mechanism of urethane: the effects on neurotransmitter-gated ion channels. *Anesth Analg* 2002; 94: 313–318.
94. Pagliardini S, Gosgnach S and Dickson CT. Spontaneous sleep-like brain state alternations and breathing

characteristics in urethane anesthetized mice. *PLoS One* 2013; 8: e70411.
95. Maggi CA and Meli A. Suitability of urethane anesthesia for physiopharmacological investigations. Part 3: other systems and conclusions. *Experientia* 1986; 42: 531–537.
96. Kramis R, Vanderwolf CH and Bland BH. Two types of hippocampal rhythmical slow activity in both the rabbit and the rat: relations to behavior and effects of atropine, diethyl ether, urethane, and pentobarbital. *Exp Neurol* 1975; 49: 58–85.
97. Bland BH and Whishaw IQ. Generators and topography of hippocampal theta (RSA) in the anaesthetized and freely moving rat. *Brain Res* 1976; 118: 259–280.
98. Vandecasteele M, Varga V, Berenyi A, et al. Optogenetic activation of septal cholinergic neurons suppresses sharp wave ripples and enhances theta oscillations in the hippocampus. *Proc Natl Acad Sci U S A* 2014; 111: 13535–13540.
99. Srejic LR, Valiante TA, Aarts MM, et al. High-frequency cortical activity associated with postischemic epileptiform discharges in an in vivo rat focal stroke model. *J Neurosurg* 2013; 118: 1098–1106.
100. Yokoyama O, Yoshiyama M, Namiki M, et al. Influence of anesthesia on bladder hyperactivity induced by middle cerebral artery occlusion in the rat. *Am J Physiol* 1997; 273: R1900–1907.
101. Sheorajpanday RV, Nagels G, Weeren AJ, et al. Reproducibility and clinical relevance of quantitative EEG parameters in cerebral ischemia: a basic approach. *Clin Neurophysiol* 2009; 120: 845–855.
102. van Putten MJ and Tavy DL. Continuous quantitative EEG monitoring in hemispheric stroke patients using the brain symmetry index. *Stroke* 2004; 35: 2489–2492.
103. Assenza G, Zappasodi F, Pasqualetti P, et al. A contralesional EEG power increase mediated by interhemispheric disconnection provides negative prognosis in acute stroke. *Restor Neurol Neurosci* 2013; 31: 177–188.
104. Di Pino G, Pellegrino G, Assenza G, et al. Modulation of brain plasticity in stroke: a novel model for neurorehabilitation. *Nat Rev Neurol* 2014; 10: 597–608.
105. Kauhanen ML, Korpelainen JT, Hiltunen P, et al. Aphasia, depression, and non-verbal cognitive impairment in ischaemic stroke. *Cerebrovasc Dis* 2000; 10: 455–461.
106. Gummow LJ, Dustman RE and Keaney RP. Cerebrovascular accident alters P300 event-related potential characteristics. *Electroencephalogr Clin Neurophysiol* 1986; 63: 128–137.
107. Polich J and Kok A. Cognitive and biological determinants of P300: an integrative review. *Biol Psychol* 1995; 41: 103–146.
108. Lisman J and Buzsaki G. A neural coding scheme formed by the combined function of gamma and theta oscillations. *Schizophr Bull* 2008; 34: 974–980.
109. Moran LV and Hong LE. High vs low frequency neural oscillations in schizophrenia. *Schizophr Bull* 2011; 37: 659–663.